Generative Adversarial Network-Based Restoration of Speckled SAR Images

Puyang Wang, *Student Member, IEEE*, He Zhang, *Student Member, IEEE*
and Vishal M. Patel, *Senior Member, IEEE*

***Abstract*—Synthetic Aperture Radar (SAR) images are often contaminated by a multiplicative noise known as speckle. Speckle makes the processing and interpretation of SAR images difficult. We propose a deep learning-based approach called, Image Despeckling Generative Adversarial Network (ID-GAN), for automatically removing speckle from the input noisy images. In particular, ID-GAN is trained in an end-to-end fashion using a combination of Euclidean loss, Perceptual loss and Adversarial loss. Extensive experiments on synthetic and real SAR images show that the proposed method achieves significant improvements over the state-of-the-art speckle reduction methods.**

***Index Terms*—Generative adversarial network, synthetic aperture radar, despecking, denoising, image restoration, perceptual loss.**

I. Introduction

Synthetic aperture radar (SAR) is a coherent radar imaging method which is able to produce high-resolution images of targets and landscapes. Due to its ability to capture images both at night and in bad weather conditions, SAR imaging has several advantages compared to optical and infrared systems. However, coherent imaging methods often suffer from multiplicative noise known as speckle [1]. Speckle is caused by the constructive and destructive interference of the coherent returns scattered by small reflectors within each resolution cell. The presence of speckle in SAR images can often make the processing and interpretation difficult for computer vision systems as well as human interpreters. Hence, it is important to remove speckle from SAR images to improve the performance of various computer vision algorithms such as segmentation, detection and recognition.

Let $Y \in \mathbb{R}^{W\times H}$ be the observed image intensity, $X \in \mathbb{R}^{W\times H}$ be the noise free image, and $F \in \mathbb{R}^{W\times H}$ be the speckle noise. Then assuming that the SAR image is an average of L looks, the observed image Y is related to X by the following multiplicative model [2]

$$Y = FX, \tag{1}$$

where F is the normalized fading speckle noise random variable. One common assumption on F is that it follows a Gamma distribution with unit mean and variance $\frac{1}{L}$ and has the following probability density function [3]

$$p(F) = \frac{1}{\Gamma(L)} L^L F^{L-1} e^{-LF}, \tag{2}$$

where $\Gamma(\cdot)$ denotes the Gamma function and $F \geq 0$, $L \geq 1$.

Various methods have been developed in the literature to suppress speckle including multi-look processing [4], [5], filtering methods [6], [7], [8], wavelet-based despecking methods [9], [10], [11], [12], block-matching 3D (BM3D) algorithm [13] and Total Variation (TV) methods [14]. Note that some of these methods apply homomorphic processing in which the multiplicative noise is transformed into an additive noise by taking the logarithm of the observed data [12]. Furthermore, due to local processing nature of some of these methods, they often fail to preserve sharp features such as edges and often contain block artifacts in the denoised image.

(a) Speckled image (b) Despeckled image

Fig. 1: Sample results of the proposed ID-GAN method for image despeckling

Recently, Convolutional Neural Network (CNN) based methods have shown to produce state-of-the-art results on various image restoration tasks such as image de-noising [15], image de-raining [16] and image super-resolution [17]. In particular, Generative Adversarial Networks (GANs) based image restoration methods have gained a lot of interest in recent years [18] [19], [20], [21]. The optimization goal of most of CNN-based image restoration algorithms is commonly the minimization of the pixel-wise Euclidean loss between the corrupted observation and the ground truth. However, due to the fact that every pixel is treated the same way and independently by the Euclidean loss, perceptually meaningful information may be lost during the optimization. Meanwhile, the discriminative information should also be taken into consideration to ensure that the despeckled image is indistinguishable from its clean one. To make sure that the restored image is indistinguishable from its clean one, an Image Despeckling Generative Adversarial Network (ID-GAN) approach is proposed in this paper.

Rather than using a homomorphic transformation [12], we directly estimate the clean image using the input images based on the observation model (1). The proposed ID-GAN method consists of a generator network G and a discriminator network D. Both subnetworks consists of several convolutional layers

978-1-5386-1251-4/17/$31.00 ©2017 IEEE

along with batch normalization [22] and rectified linear unit (ReLU) [23] activation function (see Figure 2). A game theoretic min-max optimization framework [18] is used to simultaneously train both G and D. The goal of GAN is to train G to produce samples from training distribution such that the synthesized samples are indistinguishable from actual distribution by the discriminator D. The generator G is trained in an end-to-end fashion using a combination of Euclidean loss, perceptual loss and adversarial loss with appropriate weights. The perceptual loss, evaluated on high-level features of G is optimized in the network to capture the perceptually meaningful detail. Meanwhile, the incorporation of the perceptual loss can also guarantee that the despeckled image is able to generate similar high-level features compared with its clean one. One of the main advantages of using deep learning-based methods for image despeckling is that they learn parameters for image restoration directly from the training data rather than relying on pre-defined image priors or filters. To the best of our knowledge, this is the first approach to image despeckling using GANs. Extensive experiments evaluated on synthetic and real SAR images show that the proposed method achieves significant improvements over the state-of-the-art speckle reduction methods.

Figure 1 shows a sample output from our ID-GAN method. Given the noisy image in Figure 1 (a), ID-GAN estimates the denoised image shown in Figure 1 (b). As can be seen by comparing Figure 1 (a) and (b), one can see that our method is able to denoise the speckled image reasonably well.

II. Proposed Method

In this section, we provide details of the proposed ID-GAN method in which we aim to learn a mapping from input speckled SAR images to despeckled images for noise removal. The proposed method consists of three main components: generator network (G), discriminator network (D) and combined loss function. The generator sub-network G is a symmetric deep CNN network with auto-encoders structure as shown in Figure 2(a). Its primary goal is to restore a despeckled image from a noisy observation. The discriminator sub-network D, as shown in Figure 2(b), serves to distinguish the de-speckled image synthesized by the generator G from the corresponding ground truth image. In other words, it provides guidance to G. Since GANs are known to be unstable to train which often results in artifacts in the output image synthesized by G, we define a refined perceptual loss function to address this issue. Additionally, the introduction of perceptual loss can also guarantee that the despeckled results preserve semantically meaningful details.

A. Network Architecture

As the goal of SAR image de-speckling is to generate pixel level de-speckled image, the generator should be able to remove speckle as much as possible without losing any detail information of the underlying clean image. So the key part lies in designing a good structure to generate de-speckled image. Inspired by some recent convolutional encoder-decoder type networks for image restoration tasks [24], we adopt a similar network for G. The combination of both convolutional and de-convolutional layers allows the network to capture the abstraction of image contents (features) while eliminating noise/corruptions through convolutional layers and hence recover the image details from features through the following de-convolutional layers.

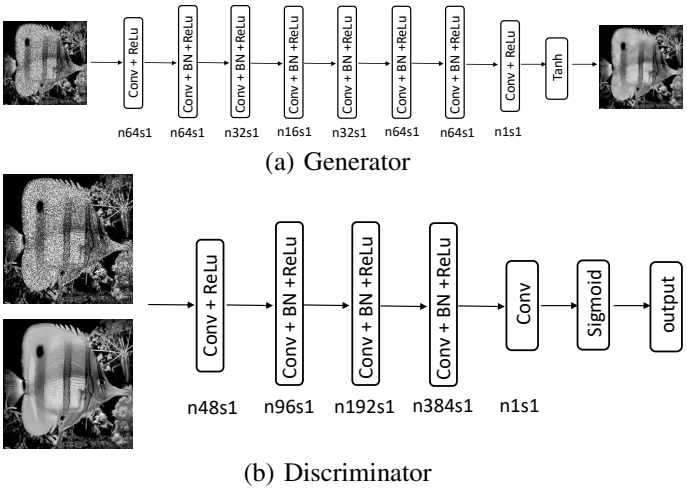

(a) Generator

(b) Discriminator

Fig. 2: Proposed ID-GAN network architecture for image despeckling.

As for the discriminator D, we follow the structure that was proposed in [25]. Once we calculate the learned features from a sequence of convolution, batch normalization and rectified linear unit (Conv-BN-ReLU) layers, a sigmoid function is stacked at the end to map the output to a probability score normalized to $[0, 1]$. The proposed discriminator sub-network D is shown in Figure 2(b). Note that the $n48s1$ in the figure stands for 48 feature maps with one stride.

B. Loss Function

In order to learn a good generator G so as to fool the learned discriminator D and to make the discriminator D good enough to distinguish synthesized despeckled image from real ground truth, the proposed method alternatively updates G and D following the structure proposed in [18]. To ensure that the results have good visual and quantitative scores along with good discriminatory performance, we propose a new refined loss function for G. Specifically, we combine the pixel-to-pixel Euclidean loss, perceptual loss and adversarial loss together with appropriate weights to form our new refined loss function. The new loss function is defined as follows

$$L = L_E + \lambda_a L_A + \lambda_p L_P, \tag{3}$$

where L_A represents adversarial loss (loss from the discriminator D), L_P is perceptual loss and L_E is the normal per-pixel Euclidean loss function. Here, λ_p and λ_a are pre-defined weights for perceptual loss and adversarial loss, respectively. If we set both λ_p and λ_a to be 0, then the network reduces to a normal CNN configuration, which aims to minimize only the Euclidean loss between the output image and the ground truth. If λ_p is set to 0, then the network reduces to a normal

GAN. And finally, if λ_a set to 0, then the network reduces to the structure proposed in [26].

The three loss functions, L_P, L_E and L_A are defined as follows. Given an image pair (X, Y), where Y is the noisy input image and X is the corresponding ground truth, the per-pixel Euclidean loss is defined as

$$L_E(\phi_G) = \frac{1}{WH}\sum_{w=1}^{W}\sum_{h=1}^{H}\|\phi_G(Y^{w,h}) - X^{w,h}\|_2^2, \quad (4)$$

where ϕ_G is the learned generator G (parameters) for generating the despeckled output and $\hat{X} = \phi_G(Y^{w,h})$. Note that we have assumed that X and Y are of size $W \times H$.

Similarly, the perceptual loss is defined as

$$L_P(\phi_G) = \frac{1}{WH}\sum_{w=1}^{W}\sum_{h=1}^{H}||V(\phi_G(Y^{w,h})) - V(X^{w,h})||_2^2, \quad (5)$$

where V represents a non-linear CNN transformation. Inspired by the idea proposed in [26], we aim to minimize the distance between high-level deep features corresponding to the output and the ground truth images using the $relu7$ layer of a pre-trained VGG16 model [27].

Finally, given a set of N despeckled images generated from the generator $\{\hat{X}_i\}_{i=1}^{N}$, the adversarial (entropy) loss computed from the discriminator that serves as a guidance to the generator is defined as

$$L_A = -\frac{1}{N}\sum_{i=1}^{N}\log(D(\hat{X}_i)). \quad (6)$$

III. Experimental Results

In this section, we present the results of our proposed ID-GAN algorithm on both synthetic and real SAR images. We compare the performance of our method with that of the following six despeckling algorithms: Lee filter [6], Kuan filter [28], PPB [29], SAR-BM3D [30], CNN [15] and SAR-CNN [31]. Note that [29], [30], [15], [31] are the most recent state-of-the-art image restoration algorithms. For all the compared methods, parameters are set as suggested in their corresponding papers. For the basic CNN method, we adopt the network structure proposed in [15] and train the network using the same training dataset as used to train our network.

To train the proposed ID-GAN, we generate a dataset that contains 3665 image pairs. Training images are collected from the UCID [32], BSDS-500 [33] and scraped Google Maps images [34] and the corresponding speckled images are generated using (1). All images are resized to 256×256. The entire network is trained using the ADAM optimization method [35], with mini-batches of size 16 and learning rate of 0.0002. During training, we set $\lambda_A = 6.6 \times 10^{-3}$ and $\lambda_P = 1$.

A. Ablation Study

We perform an ablation study to demonstrate the effects of different losses in the proposed method. Each of the losses are added one by one to the network and the results for each configuration is compared. In the first configuration, only L_E loss is minimized to train the network. The number of looks, L, is set equal to 1 and the corresponding noisy image is shown in Figure 3 (a). The restored image is shown in Figure 3 (b). It can seen that most of the speckle is removed from the noisy image, however, the denoised image still suffers from over-smoothness and fine details are missing. When the network is trained by minimizing both Euclidean and adversarial losses, more sharp edges are preserved in the result, as shown in Figure 3 (d). However, some artifacts are still present in the results. Finally, the use of our refined loss (6) removes those unwanted artifacts present in Figure 3 (c) and generates sharper edges than Figure 3 (b). This can be clearly seen by comparing Figure 3 (d) with (b) and (c). Meanwhile, the introduction of perceptual loss in the network helps to preserve fine details in the output. This experiment clearly shows the significance of having all three losses in our framework.

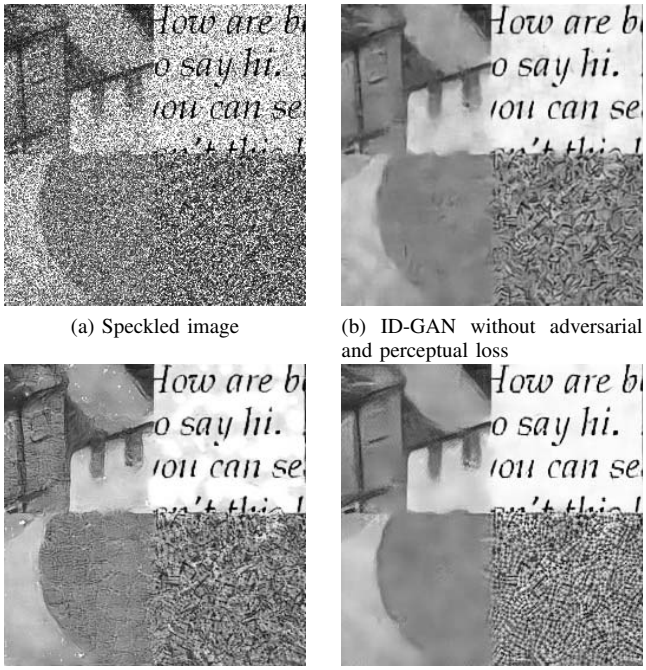

(a) Speckled image (b) ID-GAN without adversarial and perceptual loss (c) ID-GAN without perceptual loss (d) ID-GAN with all 3 losses

Fig. 3: Sample results of the proposed ID-GAN with and without adversarial and perceptual losses.

B. Results on Synthetic Images

We randomly selected 85 speckled images out of the 3665 images as the testing dataset. The remaining 3580 images are used for training the network. Experiments are carried out on three different noise levels. In particular, the number of looks L is set equal to be 1, 4 and 10, respectively. The Peak Signal to Noise Ratio (PSNR), Structural Similarity Index (SSIM) [36], Universal Quality Index (UQI) [37] and VGG16 feature loss (VGG16) [1] are used to measure the denoising performance of different methods. Results corresponding this experiment are shown in Table I. As can be seen from this table, ID-GAN provides very promising performance compared to the other

[1]VGG16 feature loss is considered as the mean square error between two features extracted at layer $relu7$ in a pre-trained VGG16 model.

Fig. 4: From left to right: SAR images, PPB, SAR-BM3D, SAR-CNN and ID-GAN.

despeckling methods in all three noise levels. Note that, for VGG16 feature loss, lower is better. Interestingly, the CNN method [15] that directly learns a mapping from a noisy input image to a clean target image using a Euclidean loss performs worse than our method and PPB [29] in many cases. This experiment clearly shows the significance of the proposed image despeckling generative adversarial network as well as the use of perceptual loss for image despeckling.

C. Results on Real SAR Images

We also evaluated the performance of the proposed method and recent state-of-the-art methods on real SAR images [38]. Since the true reflectivity fields are not available, we use the Equivalent Number of Looks (ENL) [39] to measure the performance of different image despeckling methods. The ENL values are estimated from the homogeneous regions (shown with red boxes in Figure 4). The ENL results are also tabulated in Table II. It can be observed from these results that the proposed ID-GAN outperforms the others compared methods in all four homogeneous blocks. These results also demonstrate that our ID-GAN method can achieve better performance in suppressing speckle in real SAR images.

When a clean reference is missing, visual inspection is another way to qualitatively evaluate the performance of different methods. The despeckled results corresponding to the real images are shown in Figure 4. The second to fifth columns of Figure 4 show the despeckled images corresponding to PPB, SAR-BM3D, SAR-CNN and ID-GAN, respectively. It can be observed that ENL results are consistent with the visual results. No obvious speckle exist in ID-GAN while PPB and SAR-CNN suffer from some noticeable artifacts. It is also evident from these figures that filter-based reconstructions such as PPB and SAR-BM3D generally generate blurry edges compared to SAR-CNN and ID-GAN.

TABLE I: Quantitative results for various experiments on synthetic images.

	Metric	Noisy	Lee	Kuan	PPB	SAR-BM3D	CNN	SAR-CNN	ID-GAN
$L = 1$	PSNR	14.53	21.48	21.95	21.74	22.99	21.04	**23.59**	23.13
	SSIM	0.369	0.511	0.592	0.619	0.692	0.630	0.640	**0.701**
	UQI	0.374	0.450	0.543	0.488	0.591	0.560	0.561	**0.607**
	VGG16	1.071	0.895	0.763	1.210	0.636	0.633	0.630	**0.480**
$L = 4$	PSNR	18.49	22.12	22.84	23.72	24.96	22.60	**26.20**	25.43
	SSIM	0.525	0.555	0.650	0.725	0.782	0.722	0.771	**0.808**
	UQI	0.527	0.485	0.594	0.605	0.679	0.648	0.688	**0.703**
	VGG16	0.677	0.713	0.599	0.718	0.390	0.412	0.375	**0.320**
$L = 10$	PSNR	20.54	22.30	23.11	24.92	26.45	23.52	27.63	**27.85**
	SSIM	0.602	0.571	0.671	0.779	0.834	0.741	0.825	**0.853**
	UQI	0.599	0.498	0.613	0.678	0.745	0.683	0.741	**0.765**
	VGG16	0.512	0.637	0.531	0.448	0.222	0.339	0.266	**0.206**

TABLE II: The estimated ENL results on real SAR images.

# chip	PPB	SAR-BM3D	CNN	SAR-CNN	ID-GAN
1	42.49	69.26	32.32	50.76	**84.06**
2	8.63	10.95	7.50	8.93	**11.24**
3	103.25	127.38	31.65	99.13	**169.17**
4	34.84	63.83	7.65	43.13	**63.89**

IV. Conclusion

We have proposed a new method for speckle reduction in SAR imagery based on GANs. Compared to nonlocal filtering and BM3D image despeckling methods, our GAN-based method, ID-GAN, generates the despeckled version of a SAR image through a single feedforward process. Results on synthetic and real SAR data show promising qualitative and quantitative results. An interesting feature of our method is that the network is designed to minimize perceptual difference between restored image and the ground truth image. Hence, the despeckled SAR images can be used as inputs to many SAR image understanding tasks such as road detection, railway detection, ship wake detection, texture segmentation for agricultural scenes and coastline detection, to obtain improved results.

Acknowledgment

This work was supported by an ARO grant W911NF-16-1-0126

REFERENCES

[1] J. W. Goodman, "Some fundamental properties of speckle," *Journal of the Optical Society of America*, vol. 66, no. 11, pp. 1145–1150, Nov 1976.

[2] F. Ulaby and M. C. Dobson, *Handbook of Radar Scattering Statistics for Terrain*. Norwood, MA: Artech House, 1989.

[3] F. T. Ulaby and M. C. Dobson, *Handbook of radar scattering statistics for terrain*. Artech House, 1989.

[4] C. Oliver and S. Quegan, *Understanding Synthetic Aperture Radar Images*. Norwood, MA: Artech House, 1998.

[5] P. Thompson, D. E. Wahl, P. H. Eichel, D. C. Ghiglia, and C. V. Jakowatz, *Spotlight-Mode Synthetic Aperture Radar: A Signal Processing Approach*. Norwell, MA, USA: Kluwer Academic Publishers, 1996.

[6] J.-S. Lee, "Speckle analysis and smoothing of synthetic aperture radar images," *Computer graphics and image processing*, vol. 17, no. 1, pp. 24–32, 1981.

[7] V. S. Frost, J. A. Stiles, K. S. Shanmugan, and J. C. Holtzman, "A model for radar images and its application to adaptive digital filtering of multiplicative noise," *IEEE Transactions on pattern analysis and machine intelligence*, no. 2, pp. 157–166, 1982.

[8] A. Baraldi and F. Parmiggiani, "A refined gamma map sar speckle filter with improved geometrical adaptivity," *IEEE Transactions on Geoscience and Remote Sensing*, vol. 33, no. 5, pp. 1245–1257, 1995.

[9] H. Xie, L. E. Pierce, and F. T. Ulaby, "Sar speckle reduction using wavelet denoising and markov random field modeling," *IEEE Transactions on Geoscience and Remote Sensing*, vol. 40, no. 10, pp. 2196–2212, Oct 2002.

[10] F. Argenti and L. Alparone, "Speckle removal from sar images in the undecimated wavelet domain," *IEEE Transactions on Geoscience and Remote Sensing*, vol. 40, no. 11, pp. 2363–2374, Nov 2002.

[11] A. Achim, P. Tsakalides, and A. Bezerianos, "Sar image denoising via bayesian wavelet shrinkage based on heavy-tailed modeling," *IEEE Transactions on Geoscience and Remote Sensing*, vol. 41, no. 8, pp. 1773–1784, Aug 2003.

[12] V. M. Patel, G. R. Easley, R. Chellappa, and N. M. Nasrabadi, "Separated component-based restoration of speckled sar images," *IEEE Transactions on Geoscience and Remote Sensing*, vol. 52, no. 2, pp. 1019–1029, Feb 2014.

[13] K. Dabov, A. Foi, V. Katkovnik, and K. Egiazarian, "Image denoising with block-matching and 3d filtering," in *Electronic Imaging 2006*. International Society for Optics and Photonics, 2006, pp. 606 414–606 414.

[14] J. M. Bioucas-Dias and M. A. T. Figueiredo, "Multiplicative noise removal using variable splitting and constrained optimization," *IEEE Transactions on Image Processing*, vol. 19, no. 7, pp. 1720–1730, July 2010.

[15] K. Zhang, W. Zuo, Y. Chen, D. Meng, and L. Zhang, "Beyond a gaussian denoiser: Residual learning of deep cnn for image denoising," *IEEE Transactions on Image Processing*, vol. 26, no. 7, pp. 3142–3155, July 2017.

[16] X. Fu, J. Huang, X. Ding, Y. Liao, and J. Paisley, "Clearing the skies: A deep network architecture for single-image rain removal," *IEEE Transactions on Image Processing*, vol. 26, no. 6, pp. 2944–2956, 2017.

[17] C. Dong, C. C. Loy, K. He, and X. Tang, "Learning a deep convolutional network for image super-resolution," in *European Conference on Computer Vision*. Springer, 2014, pp. 184–199.

[18] I. Goodfellow, J. Pouget-Abadie, M. Mirza, B. Xu, D. Warde-Farley, S. Ozair, A. Courville, and Y. Bengio, "Generative adversarial nets," in *Advances in neural information processing systems*, 2014, pp. 2672–2680.

[19] D. Pathak, P. Krahenbuhl, J. Donahue, T. Darrell, and A. A. Efros, "Context encoders: Feature learning by inpainting," *arXiv preprint arXiv:1604.07379*, 2016.

[20] C. Ledig, L. Theis, F. Huszár, J. Caballero, A. Cunningham, A. Acosta, A. Aitken, A. Tejani, J. Totz, Z. Wang *et al.*, "Photo-realistic single image super-resolution using a generative adversarial network," *arXiv preprint arXiv:1609.04802*, 2016.

[21] H. Zhang, V. Sindagi, and V. M. Patel, "Image de-raining using a conditional generative adversarial network," *arXiv preprint arXiv:1701.05957*, 2017.

[22] S. Ioffe and C. Szegedy, "Batch normalization: Accelerating deep network training by reducing internal covariate shift," *arXiv preprint arXiv:1502.03167*, 2015.

[23] A. Krizhevsky, I. Sutskever, and G. E. Hinton, "Imagenet classification with deep convolutional neural networks," in *Advances in neural information processing systems*, 2012, pp. 1097–1105.

[24] X. Mao, C. Shen, and Y.-B. Yang, "Image restoration using very deep convolutional encoder-decoder networks with symmetric skip connections," in *Advances in Neural Information Processing Systems*, 2016, pp. 2802–2810.

[25] A. Radford, L. Metz, and S. Chintala, "Unsupervised representation learning with deep convolutional generative adversarial networks," *arXiv preprint arXiv:1511.06434*, 2015.

[26] J. Johnson, A. Alahi, and L. Fei-Fei, "Perceptual losses for real-time style transfer and super-resolution," in *European Conference on Computer Vision*. Springer, 2016, pp. 694–711.

[27] K. Simonyan and A. Zisserman, "Very deep convolutional networks for large-scale image recognition," *arXiv preprint arXiv:1409.1556*, 2014.

[28] D. T. Kuan, A. A. Sawchuk, T. C. Strand, and P. Chavel, "Adaptive noise smoothing filter for images with signal-dependent noise," *IEEE transactions on pattern analysis and machine intelligence*, no. 2, pp. 165–177, 1985.

[29] C.-A. Deledalle, L. Denis, and F. Tupin, "Iterative weighted maximum likelihood denoising with probabilistic patch-based weights," *IEEE Transactions on Image Processing*, vol. 18, no. 12, pp. 2661–2672, 2009.

[30] S. Parrilli, M. Poderico, C. V. Angelino, and L. Verdoliva, "A nonlocal sar image denoising algorithm based on llmmse wavelet shrinkage," *IEEE Transactions on Geoscience and Remote Sensing*, vol. 50, no. 2, pp. 606–616, 2012.

[31] G. Chierchia, D. Cozzolino, G. Poggi, and L. Verdoliva, "Sar image despeckling through convolutional neural networks," *arXiv preprint arXiv:1704.00275*, 2017.

[32] G. Schaefer and M. Stich, "Ucid: An uncompressed color image database," *Storage and retrieval methods and applications for multimedia*, vol. 5307, pp. 472–480, 2004.

[33] P. Arbelaez, M. Maire, C. Fowlkes, and J. Malik, "Contour detection and hierarchical image segmentation," *IEEE Trans. Pattern Anal. Mach. Intell.*, vol. 33, no. 5, pp. 898–916, May 2011. [Online]. Available: http://dx.doi.org/10.1109/TPAMI.2010.161

[34] P. Isola, J.-Y. Zhu, T. Zhou, and A. A. Efros, "Image-to-image translation with conditional adversarial networks," *arXiv preprint arXiv:1611.07004*, 2016.

[35] D. Kingma and J. Ba, "Adam: A method for stochastic optimization," *arXiv preprint arXiv:1412.6980*, 2014.

[36] Z. Wang, A. C. Bovik, H. R. Sheikh, and E. P. Simoncelli, "Image quality assessment: from error visibility to structural similarity," *IEEE transactions on image processing*, vol. 13, no. 4, pp. 600–612, 2004.

[37] Z. Wang and A. C. Bovik, "A universal image quality index," *IEEE signal processing letters*, vol. 9, no. 3, pp. 81–84, 2002.

[38] I. Cumming and F. Wong, *Digital Processing of Synthetic Aperture Radar Data: Algorithms and Implementation*. Norwood, MA: Artech House, 2005.

[39] J.-S. Lee, "Speckle analysis and smoothing of synthetic aperture radar images," *Computer Graphics and Image Processing*, vol. 17, no. 1, pp. 24–32, Sep 1981.